

Determining the reactivity of reduced components in Dutch aquifer sediments

NIELS HARTOG

Department of Earth Sciences, Utrecht University, PO Box 80021, 3508 TA Utrecht, The Netherlands

e-mail: nhartog@geo.uu.nl

JASPER GRIFFIOEN

Netherlands Institute of Applied Geosciences-TNO National Geological Survey, PO Box 6012, 2600 JA Delft, The Netherlands

PIM F. VAN BERGEN & CORNELIS H. VAN DER WEIJDEN

Department of Earth Sciences, Utrecht University, PO Box 80021, 3508 TA Utrecht, The Netherlands

Abstract Sediments from a single aquifer were incubated under atmospheric conditions for 54 days to determine the reactivity of reductants present. The stoichiometric relationships between O₂ consumption and CO₂ production were used to evaluate the relative importance of ongoing redox processes. Respiration of bulk organic matter (BOM) and pyrite oxidation were the major processes occurring, but there was also evidence of siderite oxidation. The rates of BOM oxidation decreased continuously during the experiment. Pyrite oxidation had a maximum in its oxidation rate during the acidification process. When the acidification was buffered by carbonate dissolution, the pyrite oxidation rates decreased continuously. More than one reductant in a sample could be oxidized simultaneously.

Keywords aquifer sediment; organic matter oxidation; pyrite oxidation; reduction reactivity; redox processes; siderite oxidation

INTRODUCTION

Obtaining a detailed insight into the natural reduction capacity of aquifers has become increasingly important over recent decades. This mainly reflects the need to assess the deterioration of groundwater quality by agricultural activities (Goodrich *et al.*, 1991) and the suitability of *in situ* (bio)remediation technologies at contaminated sites (Barcelona & Holm, 1991). In the context of reaching the European objective for nitrate produced from agricultural activities (EU, 1991), recent discussions on the capacity of Dutch aquifers to reduce nitrate, have emphasized the role of pyrite and to a lesser extent that of bulk organic matter in aquifer sediments. The purpose of the present study was to assess the variability in reduction capacity of aquifer sediment by experimentally determining the relative importance of the reactive reductants present.

EXPERIMENTAL PROCEDURES

Sample collection and processing

Six core samples were taken from a borehole in a calcareous aquifer at the De Steeg drinking water production site near Langerak, The Netherlands (Table 1). This unit is

Table 1 Short description of the aquifer samples used in the incubation experiment.

Depth* (m)	<63 μm (wt. %)	63–2000 μm (wt. %)	<2 mm (wt. %)	>2 mm (wt. %)	C _{org} (wt. %)	S (wt. %)	Carbonate (wt. %)	Geological formation [†]
15.00	0.63	99.37	83.78	16.22	0.06	0.01	2.04	Kreftenheye
20.00	0.39	99.61	99.79	0.21	0.05	0.01	4.32	Kreftenheye
25.00	0.69	99.32	99.57	0.43	0.05	0.12	1.00	Urk
30.00	0.77	99.23	99.93	0.07	0.07	0.15	0.79	Urk
35.00	1.83	98.18	98.84	1.16	0.06	0.10	1.30	Sterksel/Kedichem
39.60	7.41	92.59	99.83	0.17	0.09	0.06	8.68	Sterksel/Kedichem

* Depth below surface level.

[†] Kreftenheye Formation = fluvio-glacial deposit, Urk Formation = fluvial deposit, Sterksel/Kedichem Formation = fluvial deposits.

confined by Lower Pleistocene clays at the bottom and Holocene clays and peats at the top. Sample depths ranged from 15 to 40 m below the surface. The samples were stored under a nitrogen atmosphere at 8°C directly after collection in the field. The sediments were separated into three particle size fractions: 0–63 μm (fine fraction), 63–2000 μm (coarse fraction) and 0–2000 μm (total fraction).

Sediment incubations

Samples were incubated under dark conditions. Twenty-five millilitres of vitamin and trace element solution were added in order to prevent inhibition due to nutrient limitation. Sample weight ranged from a few grammes for the fine fraction to 100 g for the total fraction. The reaction chambers (Duran 100 ml-bottle) were connected to the closed circuit of a respirometer (Micro-Oxymax™, Columbus Instruments). Carbon dioxide (CO₂) and oxygen (O₂) levels in the headspaces of the reaction chambers were kept at atmospheric conditions at 25°C ($\pm 1^\circ\text{C}$). The O₂ and CO₂ concentrations were measured every 3 h for 54 days, using an infrared sensor and an oxygen battery (fuel cell), respectively. The reaction chambers were gently shaken (100 rpm) to ensure a well-mixed chemical system.

Directly after the end of the experiment, the pH and the alkalinity of the water in the reaction chambers were measured using a standard field set. Dissolved cations and sulphate were analysed using ICP-MS. X-ray fluorescence (XRF) was used to study the bulk chemistry of the sediments. Mineralogical composition was examined by differential thermal analysis (DTA), thermogravimetry (TG) and X-ray diffraction (XRD). Carbonate and pyrite contents were determined by wet chemical analyses. The organic carbon content was determined using a C/N elemental analyser, while the particle size distribution was obtained by laser diffraction.

RESULTS AND DISCUSSION

Total reduction capacity

The cumulative O₂ consumption after 54 days (Fig. 1) can be taken as a measure of the total reduction capacity (TRC) of the samples, because the final O₂ consumption rates

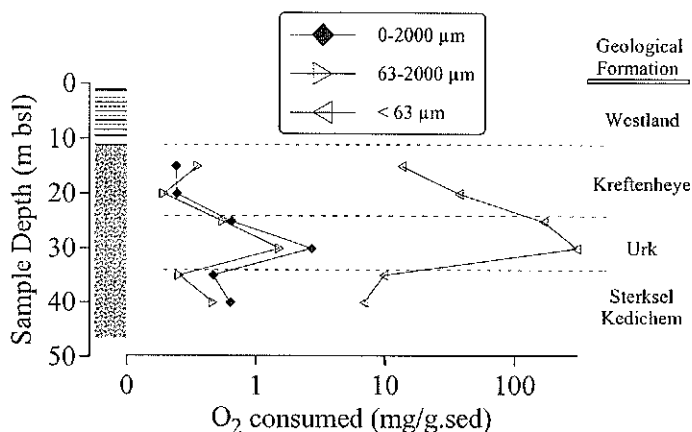


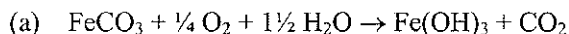
Fig. 1 Depth profile of total O₂ consumption of the different size fractions.

approached zero. This O₂ consumption of the total fractions is lowest in the samples taken from the Kreftenheye Formation, intermediate in those taken from the Sterksel/Kedichem Formation and highest in those taken from the Urk Formation. This trend is also reflected in the total O₂ consumption of the coarse and fine fractions (Fig. 1). Furthermore, the O₂ consumption of the fine fractions is up to 100 times higher than that of the corresponding total fractions. However, in this study, the absolute importance of the fine fraction is limited because it constitutes less than 2% of the total grain size distribution, except for the deepest sample (Table 1). The coarse fraction mainly acts as a dilutant of the reduction activity of the fine fraction.

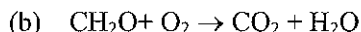
Contribution of siderite, bulk organic matter and pyrite to the TRC.

Siderite, bulk organic matter (BOM) and pyrite are potentially important O₂ consumers in the aquifer samples studied. The following redox reactions for these components are considered:

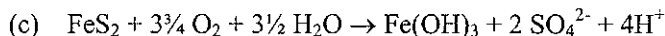
siderite



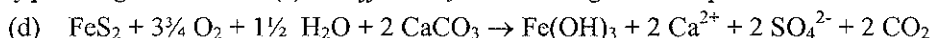
bulk organic matter simplified as CH₂O



pyrite



and if proton generation in (c) is buffered by maintaining calcite equilibrium,



It should be noted that the molar ratios of CO₂ produced to O₂ consumed are distinctly different for reactions (a)–(d). Siderite, BOM, pyrite and buffered pyrite oxidation yield a CO₂ to O₂ ratio of 4, 1, 0 and 8/15 respectively. The relative contribution of the components considered to the total O₂ consumption can be estimated using these ratios.

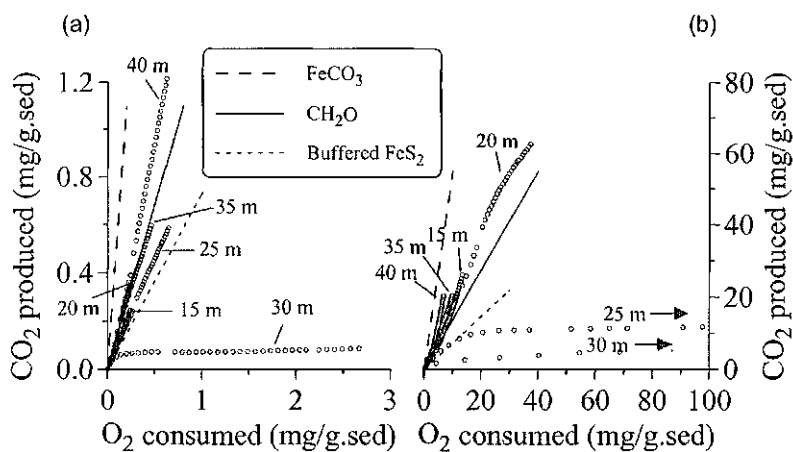


Fig. 2. Oxidation experiments. (a) Cumulative O₂ consumption vs cumulative CO₂ production during 54 days of incubation of the total fraction (0–2000 μm) samples. For reasons of clarity, the data plotted are every tenth data point available. Stoichiometric lines are plotted according to reactions (a), (b) and (d) (see text for explanation). (b) Same as (a) except for the fine fraction (0–63 μm) total O₂ consumption for 25 m: 167 mg g⁻¹ sediment, for 30 m: 299 mg g⁻¹ sediment.

Figure 2(a) shows the O₂ consumption versus the CO₂ production in the total fractions. The slopes of the cumulative O₂/CO₂ fall in the range of stoichiometries for the reactions (a)–(d). The O₂/CO₂ of the total fractions from 20 and 35 m depth only suggest the oxidation of BOM, i.e. reaction (b), while the total fractions from 15 and 25 m depth indicate the oxidation of both BOM and pyrite, i.e. reactions (b) and (d). The total fraction sample from 30 m deep initially shows pyrite oxidation with CO₂ production and O₂ consumption according to reaction (d), and subsequently O₂ consumption without CO₂ production, according to reaction (c). This indicates that the carbonate buffering is limited. The total fraction sample from 40 m deep shows a CO₂/O₂ ratio higher than that for BOM oxidation, thus part of the O₂ consumption must be caused by the oxidation of siderite. The presence of siderite in this sediment was later confirmed by DTA.

Significant differences occur between oxidation reactions in the total (Fig. 2(a)) and fine (Fig. 2(b)) fractions. For example, the CO₂/O₂ ratios of the oxidation reactions in the fine fractions (Fig. 2(b)) from 15, 20, 35 and 40 m depth are closer to the stoichiometric line for siderite oxidation than the corresponding total fractions, suggesting a greater importance of siderite oxidation in these fine fractions. Furthermore, when excluding the total fraction samples that show pyrite oxidation, the sample from 40 m depth consumed most O₂, while of the corresponding fine fractions, the sample from 20 m depth is most reactive. Finally, the pyrite oxidation in the fine fraction from 25 m depth is largely unbuffered by carbonate dissolution, while the corresponding total fraction shows buffered pyrite oxidation. This indicates that the carbonate buffer is largely contained in the coarse fraction.

The relative contribution of the different components was calculated from the resulting CO₂/O₂ ratio at the end of the incubation (Table 2). The interpretations based on the CO₂/O₂ ratios are confirmed by the pH and sulphate measurements in the water

Table 2 Measured CO₂/O₂ ratios, pH and sulphate (NA = not analysed) concentrations and calculated relative contributions of reactions (a–d) to the total O₂ consumption of the total fraction samples.

Depth (m)	(CO ₂ /O ₂) _{end} (molar)	Relative contribution of oxidation reactions (a)–(d)				pH _{end}	sulphate _{end} (mmol l ⁻¹)
		(a)	(b)	(c)	(d)		
15.00	0.75		0.46		0.54	7.2	4.4
20.00	1.06	0.02	0.98			7.5	1.7
25.00	0.66		0.27		0.73	6.3	12.7
30.00	0.02			0.96	0.04	2.1	34.0
35.00	0.94		0.87		0.13	6.8	NA
39.60	1.41	0.14	0.86			7.1	5.0

at the end of the incubations. The samples that show pyrite oxidation have high sulphate concentrations. The final pH of the sample from 30 m depth, which shows unbuffered pyrite oxidation, was 2.1. The final pH values of the other sediment incubations were near neutral (Table 2).

Kinetics and oxidation rates of the reducing components

Figure 3(a) shows the difference in the typical evolution of O₂ consumption rates between BOM and pyrite oxidation without carbonate buffering. The rates of BOM and buffered pyrite oxidation decreased continuously during the experiment. Decreasing rates for BOM oxidation are often observed (e.g. Kristensen *et al.*, 1995) and can be explained by an increasing stability of the organic compounds remaining (Cowie *et al.*, 1992; Hulthe *et al.*, 1998). Iron hydroxides, produced during buffered pyrite oxidation, may precipitate as a diffusion layer on the pyrite surfaces, slowing its oxidation (e.g. Nicholson *et al.*, 1990). The rates of unbuffered pyrite oxidation started to increase after one week, following cessation of CO₂ production once the carbonate

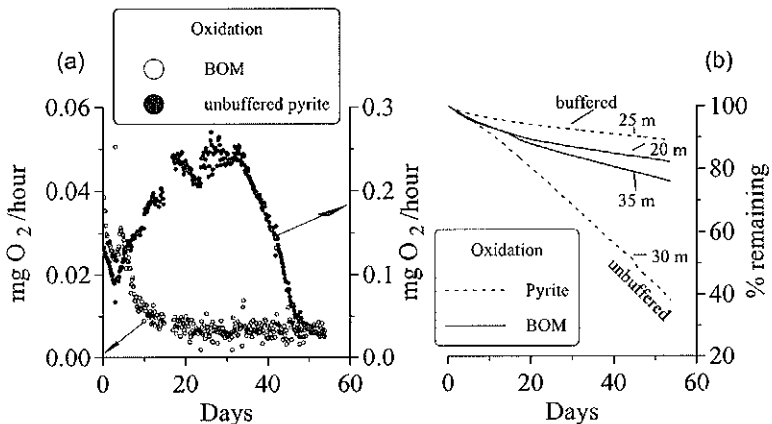


Fig. 3 Kinetics. (a) Oxygen consumption rate for the fine fractions from 20 and 25 m depth. All data points are shown. (b) Oxidation rates of selected components in four total fractions. Initial contents: 15 m: 0.06 C%, 25 m: 4272 ppm FeS₂, 30 m: 4350 ppm FeS₂, 35 m: 0.06 C%.

buffer had been consumed. Then the rates dropped off until the end of the experiment when the samples had acidified to a pH < 2. Since only the samples that showed unbuffered pyrite oxidation exhibit this typical sequence, we interpret this maximum in the O₂ consumption rate to be a pH effect. The dissolution of an inhibiting iron hydroxide coating on the pyritic surface at low pH and the subsequent release of ferric ions, that are important intermediates in the oxidation of pyrite by O₂ (Moses *et al.*, 1987), are probable causes for the increased rates. We suggest that the subsequent decrease in rates at lower pH is due to the decreasing rate of the of ferrous iron oxidation, which is the overall controlling process (Moses *et al.*, 1991)

The oxidative loss of reductants in four samples is shown in Fig. 3(b). In these samples, there was a main oxidative process (reactions a–d) responsible for the observed O₂ consumption (Table 2). The relative amounts of reductant from the sediment analyses and the cumulative O₂ consumption were calculated. The samples from 20 and 35 m depth showed oxidation of BOM. Assuming no inert organic fraction, a first order degradation model can be used:

$$dBOM/dt = -k \times BOM$$

half-lives for the BOM present were estimated to be 214 and 141 days. These oxidation rates were higher than the buffered but lower than the unbuffered pyrite oxidation rates in the samples from 25 and 30 m depth, respectively. Clearly, the buffered oxidation of pyrite in the sample from 25 m depth is slower than the oxidation of the pyrite in the sample from 30 m depth, in which half of the pyrite was oxidized in 45 days. The difference in rate between buffered and unbuffered pyrite oxidation is probably due to the precipitation of iron hydroxides on the pyrite surfaces during buffered pyrite oxidation (Nicholson *et al.*, 1990). The effect of the precipitation of an iron hydroxide coating on the oxidation of pyrite can be described (results not shown) by a shrinking core model (cf. Nicholson *et al.*, 1990). During unbuffered pyrite oxidation, however, these precipitated iron hydroxides may re-dissolve again during acidification and thus facilitate enhanced pyrite oxidation.

CONCLUSIONS

Our oxidation experiments showed the presence of BOM, pyrite and siderite as reactive reductants within a single hydrological unit. Our results clearly show that, if present, these reductants can be oxidized simultaneously. Both the TRC and the reductants that are responsible for the O₂ consumption seem to be related to the geological provenance and/or history of the sediment. The TRC of the total fractions (0–2000 µm) taken from this single aquifer unit varies by about 10 times. In these sediments, the fine fraction (0–63 µm) is about 100 times more reactive than the coarse fraction (63–2000 µm), but, because of the small amount of the fine fraction present, this has a limited effect on the reactivity of the total fraction. The coarse fraction mostly dilutes the reactivity of the fine fraction, but seems to be important in providing acid buffering capacity. This spatial heterogeneity in reactivity complicates hydrogeochemical modelling of the oxidation in a single aquifer system, since different reactions happen concurrently.

REFERENCES

- Barcelona, M. J. & Holm, R. T. (1991) Oxidation-reduction capacities of aquifer solids. *Environ. Sci. Technol.* **25**, 1565–1572.
- Cowic, G. L., Hedges, J. I. & Calvert, S. E. (1992) Sources and relative reactivities of amino acids, neutral sugars, and lignin in an intermittently anoxic marine environment. *Geochimica et Cosmochimica Acta* **56**, 1963–1978.
- European Union (EU) (1991) *Council Directive 91/676/EEC* of 12 December 1991.
- Goodrich, J. A., Lykins, Jr, B. W. & Clark, R. M. (1999) Drinking water from agriculturally contaminated groundwater. *J. Environ. Qual.* **91**, 217–235.
- Hulthe, G., Hulth, S. & Hall, P. O. J. (1998) Effect of oxygen on degradation rate of refractory and labile organic matter in continental margin sediments. *Geochimica et Cosmochimica Acta* **62**(8), 1319–1328.
- Kristensen, E., Ahmed, S. I. & Devol, A. H. (1995) Aerobic and anaerobic decomposition of organic matter in marine sediments: which is fastest? *Limnol. Oceanogr.* **40**(8), 1430–1437.
- Moses, C. O., Nordstrom, D. K., Herman, J. S. & Mills, A. L. (1987) Aqueous pyrite oxidation by dissolved oxygen and by ferric iron. *Geochimica et Cosmochimica Acta* **51**, 1561–1571.
- Moses, C. O. & Herman, J. S. (1991) Pyrite oxidation at circumneutral pH. *Geochimica et Cosmochimica Acta* **55**, 474–482.
- Nicholson, R. V., Gillham, R. W. & Reardon, E. J. (1990) Pyrite oxidation in carbonate-buffered solution: 2. Rate control by oxide coatings. *Geochimica et Cosmochimica Acta* **54**, 395–402.